DBGDGM: Dynamic Brain Graph Deep Generative Model

Alexander Campbell [1,2*] Simeon Spasov [1, 3*] Nicola Toschi [4] Pietro Liò [1]

[1]Department of Computer Science, University of Cambridge [2]The Alan Turing Institute [3]German Center for Neurodegenerative Diseases [4]Department of Biomedicine and Prevention, University of Rome Tor Vergata *Equal Contribution

MIDL Nashville 2023

Overview

- Existing methods for dynamic brain graph (DBG) representation primarily focus on node and graph embeddings, often neglecting intermediate structural elements such as node clusters.
- We introduce DBGDGM, a deep generative model that learns evolving node, community, and graph embeddings from DBGs, surpassing current standards in graph reconstruction, dynamic link prediction, and classification.

Problem formulation

- Let $\mathcal{G}^{(1:S,\,1:T)}$ denote a dataset of multi-subject DBGs derived from fMRI data. Each graph snapshot $\mathcal{G}^{(s,\,t)}$ is a non-attributed, unweighted, and undirected DBG for the s^{th} subject at the t^{th} timepoint.
- Every subject in S shares a common set of nodes $\mathcal{V}$, symbolizing brain regions, and every snapshot $\mathcal{G}^{(s,\,t)}$ consists of this node set and a distinct, time-variant edge set $\mathcal{E}^{(s,\,t)}$. Each edge, $e_i^{(s,\,t)}$ denotes a connection from source node $w_i^{(s,t)}$ to target node $c_i^{(s,t)}$, with edge numbers varying across subjects and time. Let $z_i^{(s,\,t)}$ denote the latent community assignment of $e_i^{(s,\,t)}$ to one of K clusters.
- Our model learns the graph, node, and community representations ($\boldsymbol{\alpha}^{(s)}$, $\boldsymbol{\phi}_{1:V}^{(s,t)}$, and $\boldsymbol{\psi}_{1:K}^{(s,t)}$ respectively) in an unsupervised manner. This allows for efficient adaptation to numerous downstream tasks.

Method

Generative model

First, for each subject $s \in S$, we sample a graph embedding from the prior $\boldsymbol{\alpha}^{(s)} \sim p_{\theta_\alpha}(\boldsymbol{\alpha}^{(s)})$ following:

$$p_{\theta_\alpha}(\boldsymbol{\alpha}^{(s)}) = \text{Normal}(\mathbf{0},\, \mathbf{I}) \tag{1}$$

Then, we iterate over timepoints t for subject s, and sample node and community embeddings following Markovian dynamics:

$$p_{\theta_\phi}(\boldsymbol{\phi}_n^{(s,t)} | \boldsymbol{\phi}_n^{(s,t-1)}) = \text{Normal}(\boldsymbol{\phi}_n^{(s,t-1)},\, \sigma_\phi \mathbf{I}) \tag{2}$$

$$p_{\theta_\psi}(\boldsymbol{\psi}_k^{(s,t)} | \boldsymbol{\psi}_k^{(s,t-1)}) = \text{Normal}(\boldsymbol{\psi}_k^{(s,t-1)},\, \sigma_\psi \mathbf{I}) \tag{3}$$

where $\boldsymbol{\phi}_n^{(s,\,0)} = \text{MLP}_{\theta_\phi}(\boldsymbol{\alpha}^{(s)})$, $\boldsymbol{\psi}_k^{(s,\,0)} = \text{MLP}_{\theta_\psi}(\boldsymbol{\alpha}^{(s)})$ is learnt from data. The parameters σ_ϕ, σ_ψ control temporal smoothness.

We iterate over each edge in $\mathcal{G}^{(s,\,t)}$ and sample edge community assignments:

$$p_{\theta_z}(z^{(s,\,t)} | w^{(s,,t)}) = \text{Categorical}(\text{Softmax}(\text{MLP}_{\theta z}(\boldsymbol{\phi}_w^{(s,\,t)}))) \tag{4}$$

Finally, we sample a linked target node $c^{(s,\,t)}$ from the distribution over the nodes of the assigned community:

$$p_{\theta_c}(c^{(s,\,t)} | z^{(s,\,t)}) = \text{Categorical}(\text{Softmax}(\text{MLP}_{\theta c}(\boldsymbol{\psi}_z^{(s,,t)}))) \tag{5}$$

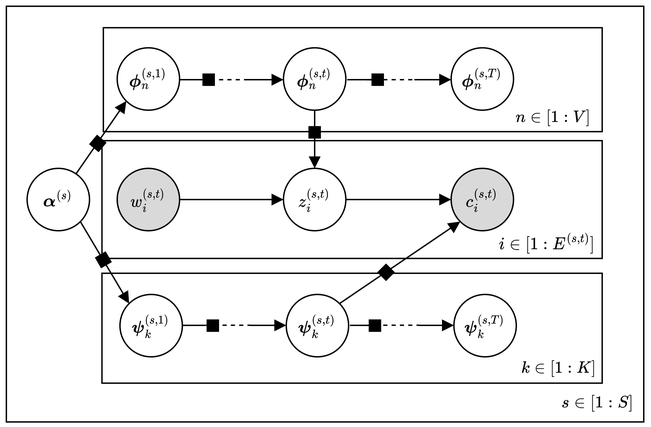

Figure: Plate diagram for DBGDGM. Latent and observed variables are denoted by white-and gray-shaded circles, respectively. Solid black squares denote non-linear mappings parameterized by NNs

Variational Inference

Inferring the true posterior p_θ is intractable. We approximate it using a variational posterior q_λ. The approximate distribution factorizes as:

$$q_\lambda = \prod_{s=1}^{S} \left(q_{\lambda_\alpha}(\boldsymbol{\alpha}^{(s)}) \prod_{t=1}^{T} \left(\prod_{n=1}^{V} q_{\lambda_\phi}(\boldsymbol{\phi}_n^{(s,t)} | \, \boldsymbol{\phi}_n^{(s,t-1)}) \right. \right. \\ \left. \left. \prod_{k=1}^{K} q_{\lambda_\psi}(\boldsymbol{\psi}_k^{(s,t)} | \, \boldsymbol{\psi}_k^{(s,t-1)}) \prod_{i=1}^{E^{(s,t)}} q_{\lambda_z}(z_i^{(s,t)} | \, \boldsymbol{\phi}_{w_i}^{(s,t)}, \, \boldsymbol{\phi}_{c_i}^{(s,t)}) \right) \right). \tag{6}$$

Moreover, each distribution is specified to mimic the structure of the generative model:

$$q_{\lambda_\alpha}(\boldsymbol{\alpha}^{(s)}) = \text{Normal}(\boldsymbol{\mu}^{(s)},\, \boldsymbol{\sigma}^{(s)}) \tag{7}$$

$$q_{\lambda_\phi}(\boldsymbol{\phi}_n^{(s,t)} | \boldsymbol{\phi}_n^{(s,t-1)}) = \text{Normal}(\tilde{\boldsymbol{\mu}}_n^{(s,t)},\, \tilde{\boldsymbol{\sigma}}_n^{(s,t)}), \quad \{\tilde{\boldsymbol{\mu}}_n^{(s,t)},\, \tilde{\boldsymbol{\sigma}}_n^{(s,t)}\} = \text{GRU}_{\lambda_\phi}(\boldsymbol{\phi}_n^{(s,t-1)}) \tag{8}$$

$$q_{\lambda_\psi}(\boldsymbol{\psi}_k^{(s,t)} | \boldsymbol{\psi}_k^{(s,t-1)}) = \text{Normal}(\tilde{\boldsymbol{\mu}}_k^{(s,t)},\, \tilde{\boldsymbol{\sigma}}_k^{(s,t)}), \quad \{\tilde{\boldsymbol{\mu}}_k^{(s,t)},\, \tilde{\boldsymbol{\sigma}}_k^{(s,t)}\} = \text{GRU}_{\lambda_\psi}(\boldsymbol{\psi}_k^{(s,t-1)}) \tag{9}$$

$$q_{\lambda_z}(z_i^{(s,t)} | \boldsymbol{\phi}_{w_i}^{(s,t)}, \, \boldsymbol{\phi}_{c_i}^{(s,t)}) = \text{Categorical}(\text{Softmax}(\boldsymbol{\pi}_i^{(s,t)})), \quad \boldsymbol{\pi}_i^{(s,t)} = \text{MLP}_{\lambda_z}(\boldsymbol{\phi}_{w_i}^{(s,t)} \odot \boldsymbol{\phi}_{c_i}^{(s,t)}) \tag{10}$$

Experiments

- **Datasets:** We use fMRI data from the Human Connectome Project (HCP) [3] and UK Biobank (UKB) [2]. We use $S = 300$ subjects evenly split between men/women, extract $V = 360$ regions-of-interest from the BOLD signal and $T = 16$ graph snapshots for each subject.
- **Baselines:** We compare against variational graph autoencoder (VGAE), a deep stochastic block model (OSBM), VGRAPH, variational graph RNN (VGRNN), Evolving Latent Space Model (ELSM), FCM, and a heuristic baseline CMN.
- **Evaluation:** Data is divided into 80/10/10% for train/valid/test along time. Graph reconstruction and link prediction are assessed on test edges, while classification (predicting biological sex) is done by passing averaged node embeddings from each subject into a SVM with 80/20% train/test split.

Results

Table: Graph reconstruction (top) and dynamic link prediction (bottom) results (mean ± standard deviation over 5 runs). First and second-best results are red and purple, respectively. Statistically significant difference from DBGDGM marked *.

Model	HCP		UKB	
	NLL (↓)	MSE (↓)	NLL (↓)	MSE (↓)
CMN	5.999 ± 0.029 *	0.050 ± 0.005 *	5.861 ± 0.017 *	0.050 ± 0.003 *
VGAE	5.857 ± 0.017 *	0.051 ± 0.002 *	5.851 ± 0.027 *	0.061 ± 0.002 *
OSBM	5.808 ± 0.026 *	0.051 ± 0.003 *	5.726 ± 0.039 *	0.052 ± 0.003 *
VGRAPH	5.569 ± 0.046 *	0.022 ± 0.004 *	5.716 ± 0.037 *	0.020 ± 0.003 *
VGRNN	5.674 ± 0.034 *	0.011 ± 0.003 *	5.649 ± 0.035 *	0.014 ± 0.002 *
ELSM	5.924 ± 0.040 *	0.081 ± 0.002 *	5.809 ± 0.024 *	0.115 ± 0.003 *
DBGDGM	4.587 ± 0.045	0.001 ± 0.002	4.586 ± 0.084	0.004 ± 0.003
	AUROC (↑)	AP (↑)	AUROC (↑)	AP (↑)
CMN	0.665 ± 0.007 *	0.654 ± 0.006 *	0.678 ± 0.004 *	0.668 ± 0.005 *
VGAE	0.661 ± 0.010 *	0.674 ± 0.008 *	0.688 ± 0.010 *	0.607 ± 0.009 *
OSBM	0.655 ± 0.027 *	0.675 ± 0.024 *	0.678 ± 0.032 *	0.682 ± 0.033 *
VGRAPH	0.689 ± 0.004 *	0.682 ± 0.002 *	0.664 ± 0.002 *	0.621 ± 0.001 *
VGRNN	0.689 ± 0.007 *	0.698 ± 0.006 *	0.698 ± 0.009 *	0.696 ± 0.007 *
ELSM	0.669 ± 0.004 *	0.662 ± 0.002 *	0.661 ± 0.001 *	0.662 ± 0.002 *
DBGDGM	0.768 ± 0.026	0.732 ± 0.032	0.786 ± 0.040	0.762 ± 0.038

- Best results on dynamic link prediction and graph reconstruction.
- Clearly, DBGDGM learns dynamic brain connectivity more effectively.

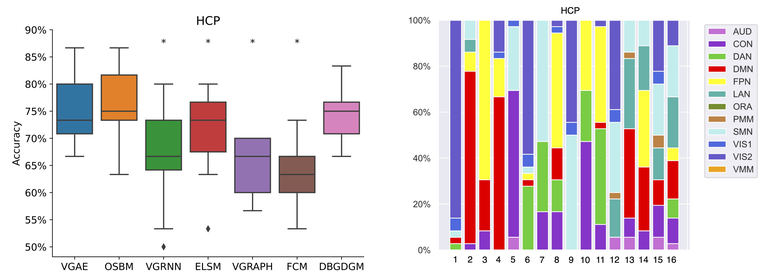

Figure: **Left:** Graph classification results (5 runs). Statistical significance from DBGDGM marked *. **Right:** Overlap between communities learned by DBGDGM and FCNs from [1]. Some communities fully correspond to known FCNs, others are a mix, and offer a way to study FCN co-activation.

- DBGDGM outperforms 4 baselines and show indiscernible performance to VGAE and OSBM.
- DBGDGM is **interpretable**. Communities which contribute most to accuracy are Cingulo-opercular (CON) and the Somatomotor (SMN) networks.

References

[1] Jie Lisa Ji, Marjolein Spronk, Kaustubh Kulkarni, Grega Repovš, Alan Anticevic, and Michael W Cole. Mapping the human brain's cortical-subcortical functional network organization. *Neuroimage*, 185:35--57, 2019.

[2] Cathie Sudlow, John Gallacher, Naomi Allen, Valerie Beral, Paul Burton, John Danesh, Paul Downey, et al. Uk biobank: an open access resource for identifying the causes of a wide range of complex diseases of middle and old age. *Plos med*, 12(3):e1001779, 2015.

[3] David C Van Essen, Stephen M Smith, Deanna M Barch, Timothy EJ Behrens, Essa Yacoub, HCP Consortium Ugurbil, et al. The wu-minn human connectome project: an overview. *Neuroimage*, 80:62--79, 2013.